# The phase behavior of charged colloidal systems in the mean spherical approximation

Simon N. Petris[a] and Derek Y. C. Chan
*Particulate Fluids Processing Centre, Department of Mathematics and Statistics, The University of Melbourne, VIC 3010 Australia*

(Received 10 December 2001; accepted 21 February 2002)

The mean spherical approximation (MSA) was used to investigate the phase behavior of charged colloidal systems with and without added salt. The competition between cohesive Coulomb interactions and stabilizing entropic and hard-core interactions controls the stability of the system and under certain circumstances, a liquid–gas-type phase transition can occur. The critical parameters and phase diagrams in the MSA obtained via the internal energy path, are compared with two-component Monte Carlo simulations and other theoretical approaches. © *2002 American Institute of Physics.* [DOI: 10.1063/1.1469606]

## I. INTRODUCTION

The phase behavior of charged colloidal systems has attracted tremendous theoretical and experimental interest in the literature over the last two decades. The traditional model for colloidal interactions is based on the Deryaguin–Landau–Verwey–Overbeek[1] (DLVO) picture, in which the colloidal dispersion is treated as a one-component fluid of colloidal particles interacting under a combination of attractive dispersion forces and repulsive electrical double layer forces. However, the observation of void formation and vapor–liquid condensation in de-ionized colloidal dispersions by Ise *et al.*[2] was believed to be evidence for the existence of a long-range effective electrostatic attractive interaction between like-charged colloids, challenging the DLVO picture. The experimental work of Grier,[3] who measured an apparent attraction between like charged colloids near a similarly charged interface, was thought to provide further evidence. However, with the explanation of Grier's measurements as a hydrodynamic effect,[4] and the observation that void formation may be due to the presence of low molecular weight charged polymers,[5] there no longer appears any justification to postulate the existence of long-range electrostatic attraction between like-charged particles.

Nonetheless, the above experimental observations have stimulated theoretical investigations based on classical Debye–Hückel (DH) like theories[6–9] and Monte Carlo (MC) simulation studies,[10,11] which show that liquid–gas phase separation is possible when the Coulombic interactions between charged colloidal particles and counterions are treated explicitly in the primitive model (PM). In other words, phase separation in charged colloidal systems arises naturally from Coulomb interactions in a two-component model. In essence, it is the one-component paradigm which necessitates an attractive interaction between like-charged colloids to achieve a liquid–gas phase separation. If the dispersion is regarded as a one-component system comprised of colloidal particles interacting via an effective pair potential, then the familiar van der Waals picture of vapor–liquid equilibrium requires the existence of an attractive interaction between the particles. Instead, one should consider the total free energy of the system which arises from Coulomb interactions between all species in the system—the Coulomb interaction between the colloidal particles, between the colloidal particles and the small ions as well as between the small ions. By focusing on the free energy of the entire system, there is in fact no conflict between the picture of a purely repulsive effective interaction between any pair of colloidal particles and the possible existence of vapor–liquid equilibrium for the whole system.

In our previous study, which followed the pioneering ideas of Langmuir[12] and the restricted primitive model (RPM) study of Fisher,[13] we showed that a liquid–gas-type phase instability is possible using extended Debye–Hückel theory. In this paper we investigate the phase behavior of charged colloidal dispersions modeled as asymmetric electrolytes using the mean spherical approximation (MSA). The MSA is instructive because it can be solved analytically in the PM. Of particular interest, are the phase diagrams of charge asymmetric electrolytes with and without added salt. In a previous MSA study, Groot[14] investigated the osmotic pressure of a colloidal dispersion relative to its supernatant in Donnan equilibrium. von Grünberg *et al.*[15] recently extended this analysis using the Poisson–Boltzmann cell model and compared predictions from the linear and nonlinear theory. Gonzalez–Tovar[16] has considered the effect of size and charge asymmetries on the MSA critical parameters of the salt-free system.

The theoretical treatment of systems involving long-ranged Coulomb interactions can be quite subtle and sometimes well-established approximations that are valid in treating systems with short-ranged potentials can lead to incorrect conclusions. The phenomenon of Coulombic phase behavior in the PM has been investigated to different degrees using other theories, and we attempt a comparison between the present work and the work of Belloni,[17,18] of van Roij

[a]Author to whom correspondence should be addressed. Electronic mail: spetris@ms.unimelb.edu.au

 

*et al.*[6,19,20] and of Warren,[7] who took similar approaches to study the phase separation problem. The general physical content invoked in explaining the phase separation phenomenon is quite similar,[21] although the technical details and findings of each approach is often significantly different.

## II. COLLOIDAL SYSTEM AS AN ASYMMETRIC ELECTROLYTE

We choose to model a de-ionized colloidal dispersion as an asymmetric electrolyte using the PM, in which the ionic species are represented as charged hard spheres with differing size and valence. For pedagogic reasons we prefer to keep the system simple to bring out the key ideas. To this end, we will consider colloidal particles of hard sphere radius $R$ and valence $Z$ that are neutralized by monovalent point counterions and any excess salt counterions and coions will also be monovalent point particles, which is strictly allowable within only DH and MSA. We assume $N_0$ colloidal particles, $N_1$ neutralizing counterions and $N_s$ added salt pairs in a volume $V$. The number density of the colloids is $n_0 = N_0/V$, of the neutralizing counterions is $n_1 = N_1/V$, of the salt coions and counterions are $n_s = N_s/V$ and the total system satisfies the bulk electroneutrality condition $\Sigma_i n_i z_i = 0$. The salt counterions and neutralizing counterions are assumed to be indistinguishable, thus the total number density of counterions is $Zn_0 + n_s$, by electroneutrality. The aqueous solvent is treated as a continuum with a relative dielectric permittivity $\varepsilon$.

The interaction potential between two ionic species $\alpha$ and $\beta$ at a distance $r$ between their centers is taken to be made up of a hard-sphere (hs) part and a Coulomb (coul) part

$$u_{\alpha\beta}(r) = u^{\mathrm{hs}}_{\alpha\beta}(r) + u^{\mathrm{coul}}_{\alpha\beta}(r), \tag{1}$$

where the hard sphere and the Coulomb interactions are given by,

$$u^{\mathrm{hs}}_{\alpha\beta}(r) = \begin{cases} \infty, & r < (R_\alpha + R_\beta), \\ 0, & r \geqslant (R_\alpha + R_\beta), \end{cases} \tag{2}$$

$$u^{\mathrm{coul}}_{\alpha\beta}(r) = \frac{z_\alpha z_\beta e^2}{\varepsilon r}, \quad r > 0 \tag{3}$$

with $e$ denoting the protonic charge.

## III. MEAN SPHERICAL APPROXIMATION

The Ornstein–Zernike (OZ) equation

$$h_{\alpha\beta}(\mathbf{r}) = c_{\alpha\beta}(\mathbf{r}) + \sum_k \int c_{\alpha k}(\mathbf{r}')\rho_k h_{k\beta}(\mathbf{r}-\mathbf{r}')d^3r' \tag{4}$$

is used to investigate fluid structure when combined with a closure approximation. The mean spherical approximation[22,23] is a closure defined by

$$\begin{aligned} h_{\alpha\beta}(r) &= -1, \quad r < (R_\alpha + R_\beta), \\ c_{\alpha\beta}(r) &= -\frac{u_{\alpha\beta}(r)}{kT}, \quad r > (R_\alpha + R_\beta) \end{aligned} \tag{5}$$

which renders the OZ equation exactly solvable for the PM, making it a convenient choice to investigate the phase behavior of asymmetric electrolytes. Hayter and Penfold[24] pointed out that a deficiency of the MSA is that it can yield negative values of radial distribution function at low densities. The parameter $2\Gamma_B$ plays the role of the inverse screening length in the MSA, and is determined by the solution of an algebraic equation. For a number density $n_0$ of colloidal particles, $n_1$ monovalent point counterions, and $n_s$ added salt with the corresponding properties of $z_0 = Z\ (>0)$, $z_1 = -1$, $z_s = \pm 1$, $R_0 = R$, and $R_1, R_s = 0$, the expression for $\Gamma_B$ which must be solved at each state point is

$$\Gamma_B^2 = \pi L_B \left( \frac{n_0 Z^2}{\left( 2\Gamma R + \frac{1+2\phi}{1-\phi} \right)^2} + n_0 Z + 2n_s \right), \tag{6}$$

where $\phi = \frac{4}{3}\pi R^3 n_0$ is the colloid volume fraction, $L_B = e^2/\varepsilon kT$ is the Bjerrum length, $k$ is the Boltzmann constant, and $T$ is the temperature.

Our starting point for considering phase behavior of charged colloidal dispersions is to calculate the internal energy, Helmholtz free energy, pressure and chemical potential of the system. The excess thermodynamic properties in the MSA for a multicomponent PM were obtained by Blum and Høye,[22] and Hiroike.[25] Applied to our specified system, the excess electrostatic internal energy per unit volume is

$$\begin{aligned} \frac{E^{\mathrm{coul}}}{VkT} = -L_B \Bigg[ & \left( \frac{n_0 Z^2}{(1+2\Gamma_B R)} + n_0 Z + 2n_s \right) \Gamma_B \\ & + \frac{2\pi n_0^2 Z^2 R^2}{(1+2\Gamma_B R)[(1-\phi)(1+2\Gamma_B R)+3\phi]} \Bigg]. \end{aligned} \tag{7}$$

The excess electrostatic Helmholtz free energy per unit volume via the energy path is then

$$\frac{F^{\mathrm{coul}}}{VkT} = \frac{E^{\mathrm{coul}}}{VkT} + \frac{\Gamma_B^3}{3\pi} \tag{8}$$

and the corresponding excess electrostatic pressure is

$$\frac{P^{\mathrm{coul}}}{kT} = -\frac{\Gamma_B^3}{3\pi} - 2\pi L_B \left[ \frac{n_m Z R}{(1-\phi)(1+2\Gamma_B R)+3\phi} \right]^2 \tag{9}$$

which is always negative. In other words, the bare Coulomb repulsion between the colloid–colloid species and between the ionic species of the same valence are outweighed by the bare Coulomb attraction between the colloid- counterion species and ions of opposite valence, with the effect that the net Coulomb interaction is cohesive and tends to destabilize the ionic system.

To analyze the phase behavior of the system one must combine the above terms with the appropriate ideal gas (id) and hard-core (hc) terms. For the free energy these are

$$\begin{aligned} \frac{F^{\mathrm{id}}}{VkT} = & n_0 \log n_0 - n_0 + n_s \log n_s - n_s \\ & + (Zn_0 + 2n_s)\log(Zn_0 + 2n_s) - (Zn_0 + 2n_s), \end{aligned} \tag{10}$$

$$\frac{F^{\mathrm{hc}}}{VkT} = n_0 \left( \frac{4-3\phi}{(1-\phi)^2} \right) + (Zn_0 + 2n_s) \log\left( \frac{1}{1-\phi} \right). \tag{11}$$

These definitions are consistent with the Carnahan–Starling formula[9] for the pressure of a system of uncharged hard sphere colloids and uncharged point ions

$$\frac{P^{\mathrm{hc,id}}}{VkT}=n_0\left(\frac{1+\phi+\phi^2-\phi^3}{(1-\phi)^3}\right)+\left(\frac{Zn_0+2n_s}{1-\phi}\right), \tag{12}$$

where the first term in (12) corresponds to hard-core interactions between the colloids and the second term is the hard-core excluded volume contribution between all the point ions and the colloids. The total system pressure is

$$P=P^{\mathrm{hc,id}}+P^{\mathrm{coul}}. \tag{13}$$

The ideal and hard-core contributions are always positive and maintain stability in the dispersion, while the Coulomb contribution is always negative and is destabilizing. The combination of these terms signals the possibility of a liquid–gas phase equilibrium when the system is in a region of phase space such that the relative magnitudes are comparable. This is essentially the same paradigm adopted by Langmuir[12] in considering phase behavior in strongly interacting dispersions.

The colloids and their neutralizing counterions are treated as one chemical species, since the density of counterions is proportional to colloid density due to electroneutrality ($n_1=Zn_0$). Neutral pairs of added salt particles are another independent species. There are then effectively two relevant chemical potentials, which shall be referred to as the colloid and salt chemical potentials. They are determined by differentiating the total free energy per unit volume with respect to the density of one species, holding the density of the other species fixed,

$$\mu_{\mathrm{col}}=\left[\frac{\partial(F^{\mathrm{tot}}/V)}{\partial n_0}\right]_{n_s},\qquad \mu_{\mathrm{salt}}=\left[\frac{\partial(F^{\mathrm{tot}}/V)}{\partial n_s}\right]_{n_0}. \tag{14}$$

## IV. CRITICAL POINTS AND PHASE DIAGRAMS WITH NO ADDED SALT

There are seven system parameters which characterize the state of a $Z$:1 asymmetric electrolyte with monovalent added salt: $Z, R, n_0, n_1, n_s, T$, and $\varepsilon$, however, not all of these are independent and the system can be entirely characterized by only four nondimensional variables. For our study, we chose these to be the colloid charge $Z$, the colloid volume fraction $\phi$, the scaled added salt $S$ concentration, and the electrostatic coupling parameter or inverse temperature $\Gamma$ [sometimes denoted as $\Gamma_{\mathrm{II}}$ (Ref. 10)], defined by

$$Z,\quad \phi\equiv\frac{4\pi R^3}{3}n_0,\quad S\equiv\frac{4\pi R^3}{3}n_s,\quad \Gamma\equiv\frac{e^2}{\varepsilon kTR}\equiv\frac{L_B}{R}. \tag{15}$$

All critical parameters and phase diagrams to follow are presented using these variables, and other parameters can be constructed from these four variables. For example, the Debye screening parameter, $\kappa_D$, for the whole system is

TABLE I. Critical parameters for the MSA. The values of $R^*$ are physical colloidal radii such that the corresponding critical temperature for the $Z$:1 electrolyte is 300 K, for water with $\varepsilon=78$.

| Asymm. Elec. $Z$:1 | MSA | | |
|---|---|---|---|
| | $\Gamma^{\mathrm{cr}}$ | $\phi^{\mathrm{cr}}$ | $R^*$ (nm) |
| 10:1 | 1.5 | 0.066 | 0.5 |
| 20:1 | 0.95 | 0.031 | 0.7 |
| 100:1 | 0.23 | $2.7\times10^{-4}$ | 3.1 |
| 500:1 | 0.046 | $4.3\times10^{-5}$ | 15 |
| 1000:1 | 0.023 | $2.1\times10^{-5}$ | 31 |
| 1400:1 | 0.017 | $1.5\times10^{-5}$ | 43 |

$$(\kappa_D R)^2=4\pi L_B(n_0Z^2+n_0Z+2n_S)R^2=3\Gamma\phi Z(Z+1)+6\Gamma S. \tag{16}$$

As a starting point, we shall consider the salt-free case ($S=0$) of only colloids and neutralizing counterions. We showed previously[9] that this case could lead to a liquid–gas-type phase instability using extended Debye–Hückel theory, when the system is below a critical temperature. This same qualitative behavior is found in the MSA, although the precise location of the critical parameters and thermodynamics is altered due to the different theoretical approximations. The physical effect of cooling the system is to simultaneously lower the entropy and increase Coulombic cohesion. When the cohesion becomes comparable in magnitude to the entropy, the system becomes unstable and a van der Waals loop appears in the total pressure.

A system can separate into two phases when there is thermodynamic equilibrium between each phase, which is when the temperature $T$, pressure $P$, and the chemical potentials for each component $\mu_i$, are the same in each phase. The colloid volume fraction versus temperature phase diagram for a system of colloids and counterions can be determined by solving the following conditions of coexistence at each scaled temperature $1/\Gamma$,

$$P(n_0^l)=P(n_0^g),\qquad \mu_{\mathrm{col}}(n_0^l)=\mu_{\mathrm{col}}(n_0^g), \tag{17}$$

where the superscript $l$ denotes the liquid or dense phase and $g$ the gas or dilute phase. Satisfying these conditions is equivalent to the Maxwell equal area construction of dividing a van der Waals loop in the pressure into two regions of equal area.

Approximate analytic expressions for the MSA critical parameters of a $Z$:1 asymmetric electrolyte, were found by solving $(\partial P/\partial V)=0=(\partial^2 P/\partial V^2)$ for $Z\gg1$:

$$\Gamma^{\mathrm{cr}}\equiv\left(\frac{e^2}{\varepsilon kTR}\right)^{\mathrm{cr}}\cong\frac{4}{(3-2\sqrt{2})Z},\qquad \phi^{\mathrm{cr}}\equiv\left(\frac{4\pi R^3}{3}n_0\right)^{\mathrm{cr}}\cong\frac{1}{48Z},\qquad \left(\frac{4\pi R^3P}{3kT}\right)^{\mathrm{cr}}\cong\frac{1}{3\times2^4},\quad (\kappa_D R)^{\mathrm{cr}}\cong\frac{1+\sqrt{2}}{2}. \tag{18}$$

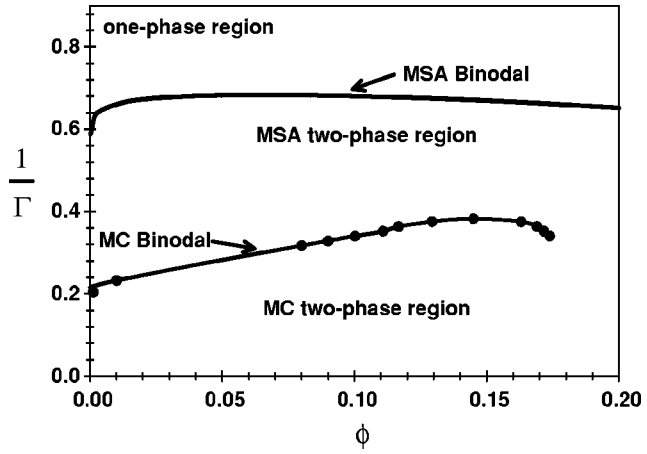


FIG. 1. Scaled temperature ($1/\Gamma = \varepsilon kTR/e^2$) vs volume fraction $\phi$ phase diagram for a 10:1 asymmetric electrolyte using the MSA and MC simulation.

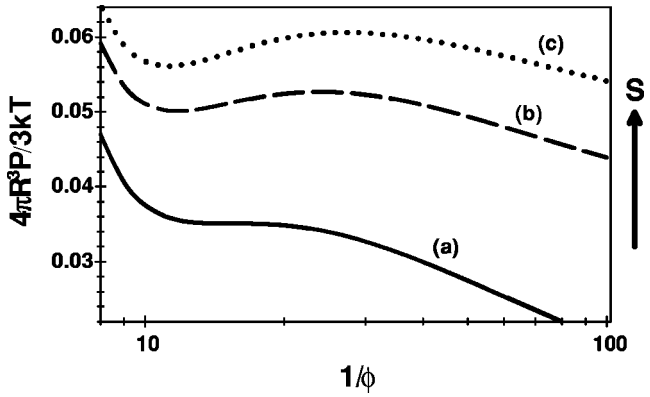


FIG. 2. Scaled pressure ($4\pi R^3 P/3kT$) vs scaled volume ($1/\phi = 3V/4\pi R^3 N_0$) diagrams for a 10:1 asymmetric electrolyte in the MSA, showing the effect of salt on the scaled pressure isotherm at $\Gamma = \Gamma^{cr} = 1.463$. The scaled salt concentrations are (a) $S = 10^{-6}$, (b) $S = 1.8 \times 10^{-2}$, (c) $S = 2.5 \times 10^{-2}$.

The exact critical parameters were determined by adjusting the coupling strength $\Gamma$ and solving the coexistence conditions in (17) numerically, to determine the binodal (coexistence) curve. The unusual feature of a second metastable critical point reported previously[9] in the extended DH theory was not found in the MSA and we believe that this feature is an artifact of DH theory. The MSA critical parameters via the energy path are shown in Table I for a range of charge asymmetries. It is also possible to determine the critical parameters in the MSA via the virial path, but the energy path is considered to be a more reliable path because it takes into account higher order terms in the pressure.[16,26] MSA critical parameters for $Z = 10$, 20, 100 were previously reported by Gonzalez-Tovar.[16]

Ideally we would like to compare the MSA critical parameters and phase diagrams with corresponding MC studies over a range of charge asymmetries. Unfortunately practical limitations relating to system size have thus far limited studies to relatively low charge asymmetries. A detailed two-component temperature and density scaling MC study of a 10:1 asymmetric electrolyte with point counterions was conducted by Reščič and Linse.[11] This regime of charge asymmetry may be found in protein solutions. They determined the critical point and phase diagram, subject to some statistical uncertainty due to system size effects. The MC critical point was found to be $\phi^{cr} = 0.14$ and $\Gamma^{cr} = 2.6$, while the MSA predicts $\phi^{cr} = 0.07$ and $\Gamma^{cr} = 1.5$ and DH[9] predicts $\phi^{cr} = 0.24$ and $\Gamma^{cr} = 0.16$.

The MSA and DH are both linear theories, which are identical in the point colloid limit. The linearization assumption is the greatest weakness of both theories. However, the MSA critical parameters are in much better agreement with MC simulation (particularly $\Gamma^{cr}$) than the DH predictions. This is probably due to the different treatment of excluded volume effects due to charged particles in each theory. In Fig. 1, the scaled temperature against colloid volume fraction phase diagram for a 10:1 asymmetric electrolyte in the MSA is compared with the MC simulation of Reščič and Linse.

The experimental studies of Ise *et al.*[1] demonstrated that stable de-ionized aqueous dispersions of polystyrene latex colloids exhibit simultaneously regions of high and low colloid densities. The exact origin of what drives this phase separation in the experiments is not known conclusively. However, it is an interesting exercise to model the experimental system as an asymmetric electrolyte to see whether the effect could be driven by cohesive Coulomb interactions. For a salt-free 1400:1 asymmetric electrolyte in water, the estimated experimental critical parameters are $\phi^{cr} \sim 10^{-4}$ and $\Gamma^{cr} \sim 0.012$, corresponding to $R_0 = 0.06\ \mu$m, $\varepsilon = 78$, and $T \sim 300$ K. Using the MSA, the predicted critical parameters are $\phi^{cr} = 10^{-5}$ and $\Gamma^{cr} = 0.017$, which suggests that Coulombic cohesion is a possible explanation for the observed phase separation.

A comparison between the MSA critical parameters, available MC critical parameters, and approximate hypernetted chain (HNC) critical parameters, is shown in Table II. The HNC critical parameters were estimated using the compressibility path by Belloni,[17,18] who points out that the HNC equation has no solution at high charge asymmetry,[18] which is why no comparison is possible for $Z = 1400$.

TABLE II. Comparison of theoretical critical parameters with simulation and experiment.

| Asymm. Elec. | MC (Refs. 10, 11) | | Expt. (Ref. 2) | | MSA | | DH (Ref. 9) | | HNC (Refs. 17, 18) | |
|---|---|---|---|---|---|---|---|---|---|---|
| $Z$:1 | $\Gamma^{cr}$ | $\phi^{cr}$ | $\Gamma^{cr}$ | $\phi^{cr}$ | $\Gamma^{cr}$ | $\phi^{cr}$ | $\Gamma^{cr}$ | $\phi^{cr}$ | $\Gamma^{cr}$ | $\phi^{cr}$ |
| 10:1 | 2.6 | 0.15 | | | 1.5 | 0.07 | 0.16 | 0.24 | ~0.54 | |
| 20:1 | ~2 | ~0.1–0.4 | | | 0.95 | 0.03 | 0.07 | 0.27 | ~0.23 | ~0.004 |
| 1400:1 | | | ~0.012 | ~$10^4$ | 0.017 | $10^{-5}$ | 0.001 | 0.33 | | |

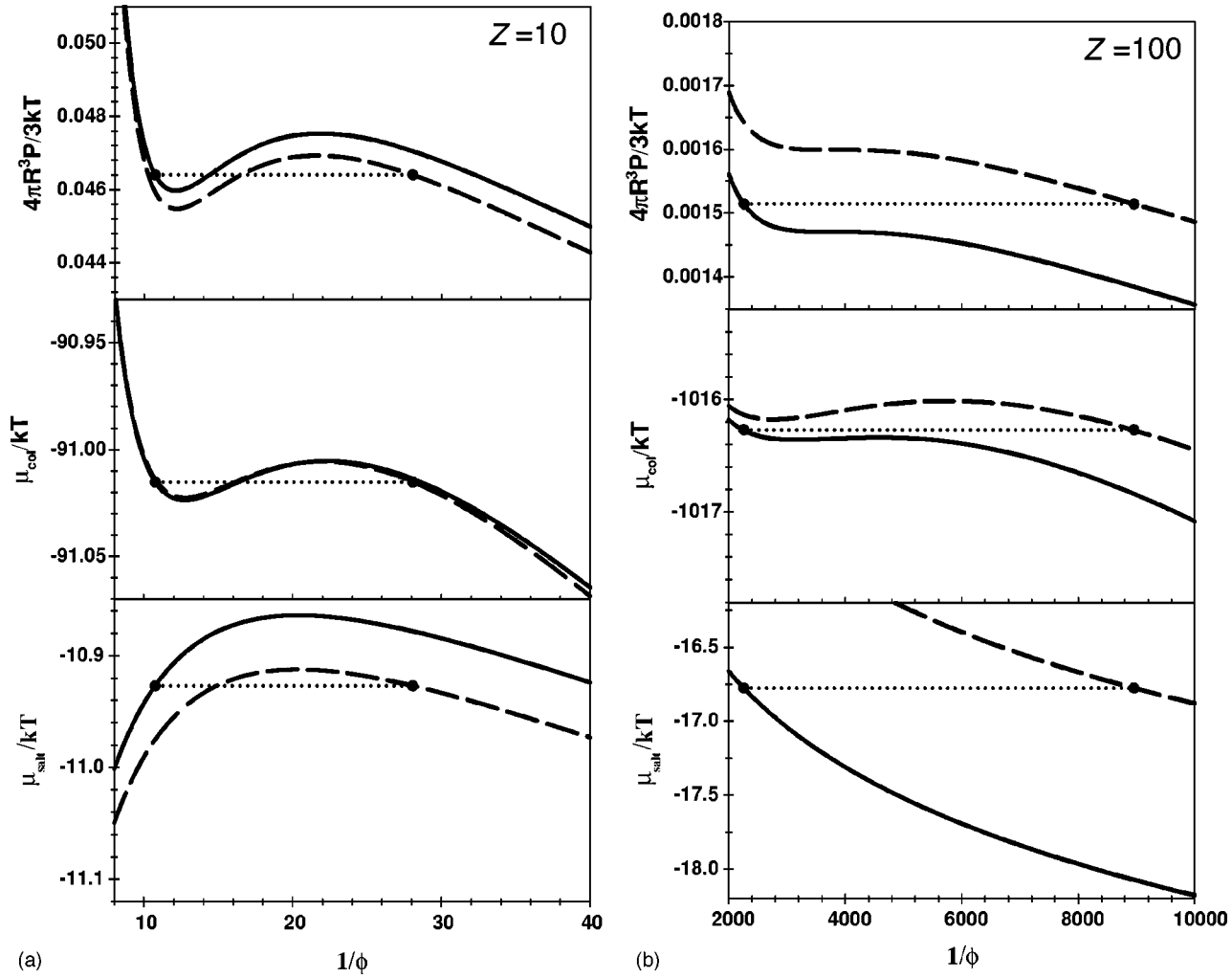


FIG. 3. (a) Pressure $P$, colloid chemical potential $\mu_{\mathrm{col}}$, and salt chemical potential $\mu_{\mathrm{salt}}$ vs scaled volume $(1/\phi = 3V/4\pi R^3 N_0)$ for a 10:1 asymmetric electrolyte in the MSA at $\Gamma = \Gamma^{\mathrm{cr}} = 1.463$. The dashed curves correspond to $S = (4\pi R^3/3)\, n_s = 0.012$, while the solid curves correspond to $S = 0.0126$. The dotted lines join the highlighted state points (•), which satisfy the coexistence conditions (19). (b) Pressure $P$, colloid chemical potential $\mu_{\mathrm{col}}$, and salt chemical potential $\mu_{\mathrm{salt}}$ vs scaled volume $(1/\pi = 3V/4\pi R^3 N_0)$ for a 100:1 asymmetric electrolyte in the MSA at $\Gamma = \Gamma^{\mathrm{cr}} = 0.226$. The dashed curves correspond to $S = (4\pi R^3/3)\, n_s = 9.2 \times 10^{-5}$, while the solid curves correspond to $S = 2.5 \times 10^{-5}$. The dotted lines join the highlighted state points (•), which satisfy the coexistence conditions (19).

Although the comparison is far from conclusive, the MSA is largely successful in predicting the trend in the critical parameters over a range in phase space compared with simulation and experiment. It is perhaps surprising that the MSA estimates of the critical parameters are in better agreement with the MC simulations, than those from the HNC. A possible explanation is the compressibility path taken to obtain the thermodynamics, because there are technical difficulties in identifying the spinodal in the HNC using compressibility path.[18] Using the energy path in the MSA, there are no such problems for any system.

## V. CRITICAL POINTS AND PHASE DIAGRAMS WITH ADDED SALT

Adding salt to an asymmetric electrolyte introduces an extra independent component which influences the phase behavior of the system. One effect of adding salt is to increase the number of particles and thus the entropic contribution to the pressure, making the system more stable. However, adding salt also increases the cohesive contribution to the pressure, which acts to destabilize the system. The net effect is determined by the relative change in magnitude of each contribution at that particular temperature. The quantitative influence of added salt on the pressure, at a temperature corresponding to the critical temperature for the salt-free system is shown in Fig. 2. When the amount of added salt is small, there is a point of inflection on the pressure isotherm. However, as more salt is added, a van der Waals loop develops and the isotherm shifts upwards to higher pressure, due to the extra entropy from the increased number of particles. With even more salt, the loop in the pressure isotherm becomes more pronounced at high density where the increase in cohesion is dominant, and flattens out at low density because the increase in entropy is dominant there.

To determine the colloid volume fraction versus added salt $(\phi - n_s)$ phase diagram at a fixed temperature $T$, the conditions of coexistence of two phases must prevail.

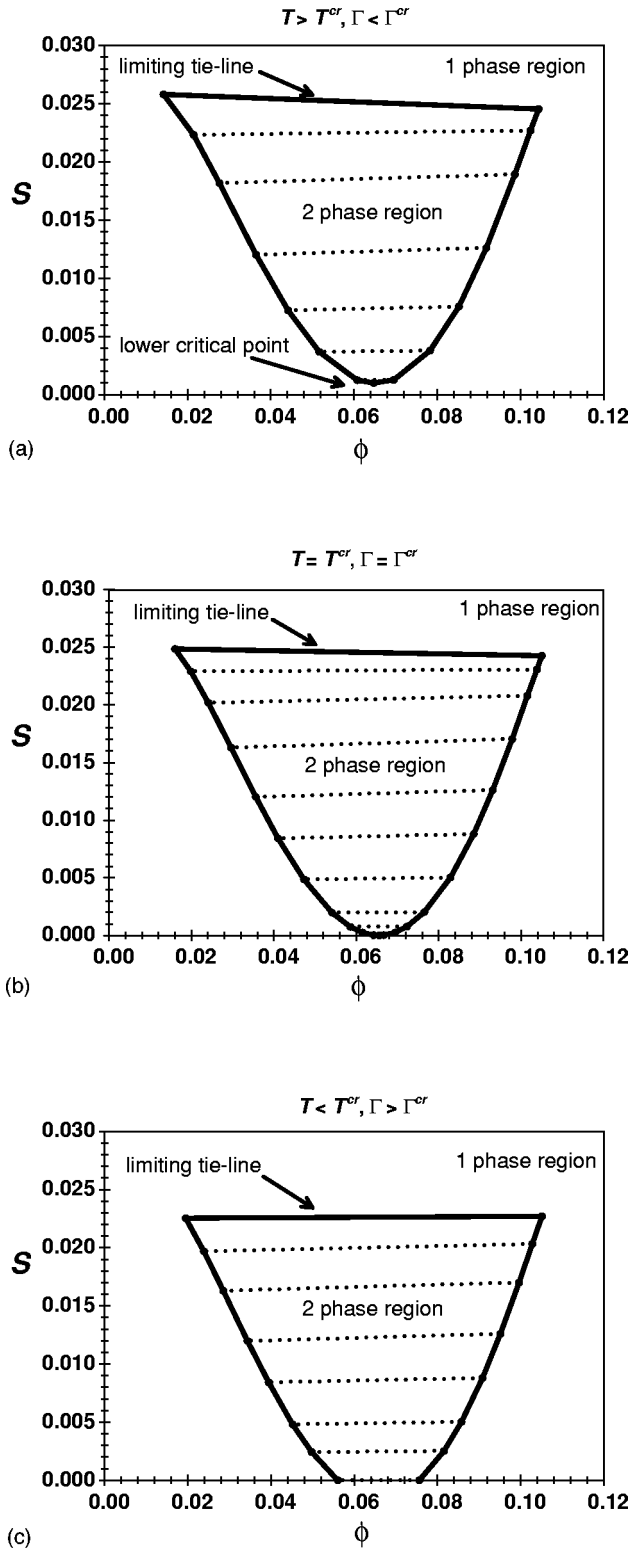


FIG. 4. Added salt $S=(4\pi R^3/3)\,n_s$ vs colloid volume fraction $\phi$ phase diagram for a 10:1 asymmetric electrolyte in the MSA at (a) $\Gamma=1.462$, (b) 1.4626 ($\Gamma^{cr}$), and (c) 1.463.

$$
\begin{aligned}
&P(n_0^l,n_s^l)=P(n_0^g,n_s^g),\\
&\mu_{\mathrm{col}}(n_0^l,n_s^l)=\mu_{\mathrm{col}}(n_0^g,n_s^g),\\
&\mu_{\mathrm{salt}}(n_0^l,n_s^l)=\mu_{\mathrm{salt}}(n_0^g,n_s^g).
\end{aligned}
\tag{19}
$$

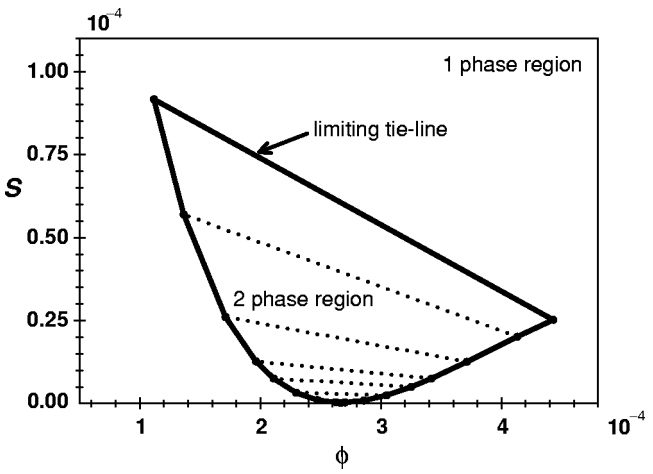


FIG. 5. Added salt $S=(4\pi R^3/3)\,n_s$ vs colloid volume fraction $\phi$ phase diagram for a 100:1 asymmetric electrolyte in the MSA at the critical temperature of the salt-free system $\Gamma=\Gamma^{cr}=0.226$.

These three equations relate four relevant densities $(n_0^l,n_s^l,n_0^g,n_s^g)$ and the phase diagram is determined by fixing the density of salt in one phase and then solving the coexistence conditions (19) to determine the three remaining densities using a root finding technique. In practice, the convergence is poor if the initial guess is far from the actual solution. It helps to begin solving the coexistence conditions for a negligibly small amount of added salt, since the colloid densities $(n_0^l,n_0^g)$ are almost identical to those in the corresponding salt-free case. One can then gradually increase the salt concentration using the previous solution as an initial guess. Eventually as more salt is added, an upper limit is reached, where the competition between entropy and cohesion cannot be balanced and the coexistence conditions (19) can no longer be satisfied. This indicates that an equilibrium two-phase system is no longer possible and the two-phase region is closed.

Figures 3(a) and 3(b) are graphical examples of coexisting phases which satisfy (19) for low and high charge asymmetries. In each example, the variation of $\mu_{\mathrm{salt}}$ differs significantly in the vicinity of criticality, which leads to the considerably different shaped phase diagrams to follow. In Fig. 3(a) with a low charge asymmetry of 10:1, $\mu_{\mathrm{salt}}$ obtains a maximum value versus scaled volume, and the concentration of salt in the dense phase is about 5% higher than in the dilute phase for coexistence. Whereas in Fig. 3(b) for high charge asymmetry, $\mu_{\mathrm{salt}}$ decreases monotonically with scaled volume, and the concentration of salt in the dilute phase is about five times higher than in the dense phase for coexistence. These observations will be made evident in the colloid volume fraction versus added salt phase diagrams.

The phase boundaries in the added salt versus colloid volume fraction phase diagram $(\phi-n_s)$ are strongly influenced by the temperature of the system relative to the critical temperature of the salt-free case. For temperatures equal to and above the salt-free critical temperature, the two-phase region resembles the lower half of a closed miscibility loop and there is a unique lower critical salt concentration. This is illustrated in the phase diagrams in Figs. 4(a) and

4(b) for a 10:1 asymmetric electrolyte. Inside the two-phase region, the system is predicted to separate into a dense and dilute colloid phase. The tie lines between points on the phase boundary indicate the relative density of colloids and salt in each phase. In Fig. 4(c), the temperature is below the salt-free critical temperature and the two-phase region appears to sink into the $\phi$ axis. There is also no longer a lower critical salt concentration because the system can phase separate without any added salt. From the alternative viewpoint, the de-ionized phase separated system can accommodate a certain amount of salt without destroying the phase coexistence.

The shape and location of the $\phi - n_s$ phase diagram seems to vary within different theoretical frameworks. Warren[7] and van Roij *et al.*[6,19,20] used variational techniques to estimate the colloid–colloid contribution to the free energy, and DH-type approximations for the colloid–ion and ion–ion contributions. They found closed miscibility loops with unique upper and lower critical salt concentrations. Since critical points correspond to inflection points in the pressure, upper and lower critical salt concentrations imply that there are two inflection points in the pressure isotherm at two different salt concentrations. The pressure in the MSA does not behave in this manner, and only a lower critical salt concentration is found.

A lower critical salt concentration is common to all the theoretical approaches, and it implies that a homogeneous de-ionized dispersion can be made to phase separate by the addition of a small amount of salt. This is perhaps counterintuitive, since it might be expected that added salt would only screen the Coulomb interactions and resist any tendency to phase separate. A possible explanation is that salt introduces an extra degree of freedom, because pairs of salt particles are neutral objects, which can accumulate in the dense or dilute phases to adjust the thermodynamic properties of the system without violating electroneutrality constraints.

In Fig. 4 for the $\phi - n_s$ phase diagram of a 10:1 asymmetric electrolyte, the tie lines are almost perfectly horizontal, indicating nearly equal salt concentrations in each phase. As mentioned earlier, this is not the case for higher asymmetries as can be seen in the phase diagrams of 100:1 (Fig. 5) and 1000:1 (Fig. 6) asymmetric electrolytes. The tie lines are sloped, indicating an excess of salt pairs in the dilute phase is required to satisfy the coexistence conditions. Essentially the dilute phase requires the extra entropy provided by the salt particles to raise the pressure and chemical potential to match that in the dense phase. Van Roij *et al.* and Warren only investigated high charge asymmetries, and they also found the same trend of higher salt concentrations in the dilute phase compared with the dense phase.

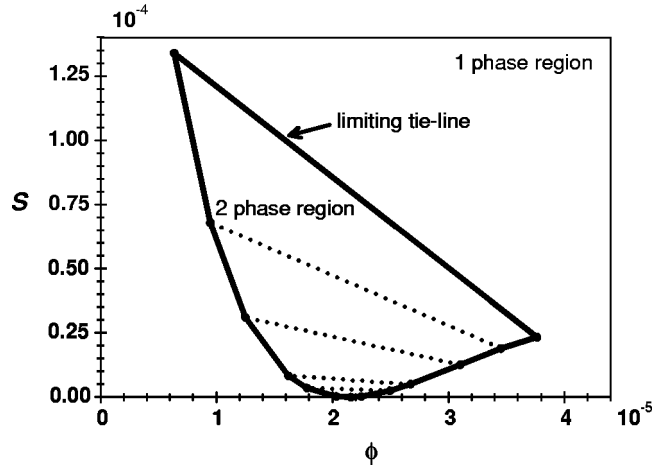


FIG. 6. Added salt $S = (4\pi R^3/3)\, n_s$ vs colloid volume fraction $\phi$ phase diagram for a 1000:1 asymmetric electrolyte in the MSA at the critical temperature of the salt-free system $\Gamma = \Gamma^{cr} = 0.226$.

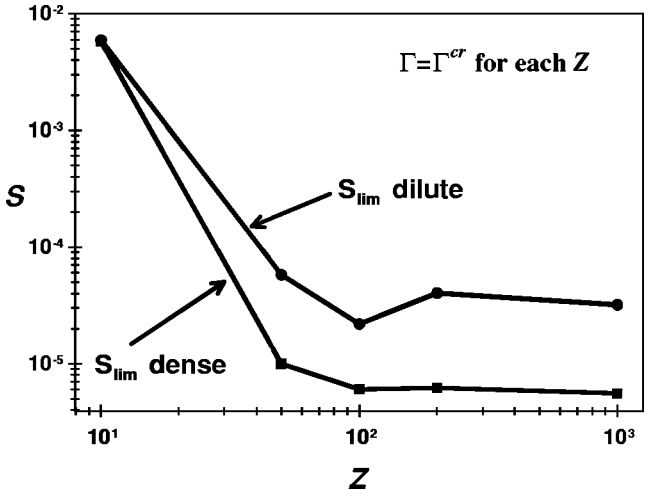


FIG. 7. Limiting scaled salt concentrations $S = (4\pi R^3/3)\, n_s$ in the dense and dilute phase vs colloid charge $Z$ over a range of charge asymmetries, at the salt-free critical temperature of each asymmetric electrolyte.

Figure 7 shows the salt concentrations in the dense and dilute phases of the limiting tie line, over a range of charge asymmetries, at the salt-free critical temperature for each system. It demonstrates that the relative amount of salt in the dilute phase compared with dense phase is almost equal for low charge asymmetries but becomes greater as the charge asymmetry increases.

## VI. CONCLUSIONS

Phase separation of a salt-free or de-ionized asymmetric electrolyte in the MSA for the PM occurs when stabilizing entropic and hard core interactions are lowered such that they are comparable in magnitude to cohesive Coulomb interactions. This is achievable by cooling the system, which simultaneously lowers the entropy and increases Coulombic cohesion in the system. When the temperature is below a critical temperature, which is dependent on the colloid charge and size, the cohesion can be significant enough to cause the system to become unstable and for a van der Waals loop to appear in the total pressure.

We have shown that adding salt to an asymmetric electrolyte increases the magnitude of both the stabilizing entropy and destabilizing Coulomb interactions and that the net effect is determined by their relative magnitudes. A de-ionized phase separated asymmetric electrolyte can accommodate a certain amount of salt without destroying the phase

coexistence. In the vicinity of criticality, a stable salt-free dispersion can be induced to phase separate by the addition of salt. This characteristic corresponds to a lower critical salt concentration in the phase diagram. For low charge asymmetries, added salt is nearly evenly distributed between the dense and dilute phase. For high charge asymmetries, added salt is more likely to be accommodated in the dilute phase rather than the dense phase.

The results in the MSA are physically instructive because it is a linear theory and its solution is analytic and transparent. However, it is possible to go beyond a linear theory by exploiting the idea of effective pair potentials between colloidal particles to include nonlinear effects in the Coulomb interaction. This will be presented in the next paper in this series.

## ACKNOWLEDGMENTS

Sincere thanks to Professor P. Linse for his critical reading of the paper and Dr. J. Reščič for valuable discussion. This research is funded in part by the Australian Research Council and their support is gratefully acknowledged.

[1] E. J. W. Verwey and J. T. G. Overbeek, *Theory of the Stability of Lyophobic Colloids* (Elsevier, Amsterdam, 1948).
[2] H. Yoshida, N. Ise, and T. Hashimoto, J. Chem. Phys. **103**, 10146 (1995).
[3] J. C. Crocker and D. G. Grier, Phys. Rev. Lett. **77**, 1897 (1996).
[4] T. M. Squires and M. P. Brenner, Phys. Rev. Lett. **85**, 4976 (2000).
[5] L. Belloni, J. Phys.: Condens. Matter **12**, R549 (2000).
[6] R. van Roij, M. Dijkstra, and J. P. Hansen, Phys. Rev. E **59**, 2010 (1999).
[7] P. Warren, J. Chem. Phys. **112**, 4683 (2000).
[8] M. Knott and I. J. Ford, Phys. Rev. E **63**, 031403 (2001).
[9] D. Y. C. Chan, P. Linse, and S. N. Petris, Langmuir **17**, 4202 (2001).
[10] P. Linse, J. Chem. Phys. **113**, 4359 (2000).
[11] J. Reščič and P. Linse, J. Chem. Phys. **114**, 10131 (2001).
[12] I. Langmuir, J. Chem. Phys. **6**, 873 (1938).
[13] M. E. Fisher, J. Stat. Phys. **75**, 1 (1994).
[14] R. D. Groot, J. Chem. Phys. **94**, 5083 (1991).
[15] H. H. von Grünberg, R. van Roij, and G. Klein, Europhys. Lett. **55**, 580 (2001).
[16] E. Gonzalez-Tovar, Mol. Phys. **97**, 1203 (1999).
[17] L. Belloni, Phys. Rev. Lett. **57**, 2026 (1986).
[18] L. Belloni, J. Chem. Phys. **98**, 8080 (1993).
[19] R. van Roij and J. P. Hansen, Phys. Rev. Lett. **79**, 3082 (1997).
[20] R. van Roij and R. Evans, J. Phys.: Condens. Matter **11**, 10047 (1999).
[21] D. Y. C. Chan, Phys. Rev. E **63**, 1806 (2001).
[22] L. Blum and J. S. Høye, J. Phys. Chem. **81**, 1311 (1977).
[23] E. Waisman and J. L. Lebowitz, J. Chem. Phys. **56**, 3086 (1972).
[24] J. B. Hayter and J. Penfold, Mol. Phys. **42**, 109 (1981).
[25] K. Hiroike, Mol. Phys. **33**, 1195 (1977).
[26] J. S. Høye and G. Stell, J. Chem. Phys. **67**, 439 (1977).